Structural, optical, and electrical properties of MgyTi1-yHx thin films

Borsa, D. M.; Gremaud, R.; Baldi, A.; Schreuders, H.; Rector, J. H.; Kooi, B.; Notten, P. H. L.; Dam, B.; Griessen, R.

Published in:
Physical Review. B: Condensed Matter and Materials Physics

DOI:
10.1103/PhysRevB.75.205408

Publication date:
2007

Structural, optical, and electrical properties of $Mg_yTi_{1-y}H_x$ thin films

D. M. Borsa,[1,*] R. Gremaud,[1] A. Baldi,[1] H. Schreuders,[1] J. H. Rector,[1] B. Kooi,[2] P. Vermeulen,[3] P. H. L. Notten,[3,4] B. Dam,[1] and R. Griessen[1]

[1]*Condensed Matter Physics, Department of Physics and Astronomy, Faculty of Sciences, Vrije Universiteit, De Boelelaan 1081, 1081 HV Amsterdam, The Netherlands*

[2]*Department of Applied Physics, University of Groningen, Nijenborgh 4, 9747 AG Groningen, The Netherlands*

[3]*Eindhoven University of Technology, 5600 MB Eindhoven, The Netherlands*

[4]*Philips Research Laboratories, 5656 AE Eindhoven, The Netherlands*

(Received 19 December 2006; published 7 May 2007)

The structural, optical, and electrical transformations induced by hydrogen absorption and/or desorption in Mg-Ti thin films prepared by co-sputtering of Mg and Ti are investigated. Highly reflective in the metallic state, the films become highly absorbing upon H absorption. The reflector-to-absorber transition is fast, robust, and reversible over many cycles. Such a highly absorbing state hints at the coexistence of a metallic and a semiconducting phase. It is, however, not simply a composite material consisting of independent MgH_2 and TiH_2 grains. By continuously monitoring the structure during H uptake, we obtain data that are compatible with a coherent structure. The average structure resembles rutile MgH_2 at high Mg content and is fluorite otherwise. Of crucial importance in preserving the reversibility and the coherence of the system upon hydrogen cycling is the accidental equality of the molar volume of Mg and TiH_2. The present results point toward a rich and unexpected chemistry of Mg-Ti-H compounds.

DOI: 10.1103/PhysRevB.75.205408 PACS number(s): 78.20.−e, 78.40.−q, 73.61.−r, 68.55.Jk

I. INTRODUCTION

Recently, Notten and co-workers[1,2] reported on the excellent hydrogen storage capacity of Mg-Ti-H thin films which is approximately five times larger than that of conventional metal hydride electrodes in NiMH batteries. Rather surprisingly, we found that the same material has also remarkable optical properties.[3] Highly reflective in the metallic state, the films become strongly absorbing upon hydrogen absorption. For example, fully hydrogenated $Mg_{0.80}Ti_{0.20}H_{\sim 1.7}$ (5.5 wt. % H) thin films combine a high absorption (87% of the solar spectrum) with a low thermal emissivity (only 10%), while after removal of hydrogen $Mg_{0.80}Ti_{0.20}$ absorb no more than 1/3 of the solar spectrum. The energy conversion performance of fully hydrogenated $Mg_{0.80}Ti_{0.20}H_{\sim 1.7}$ is comparable to those of advanced solar coatings such as ceramic-metal composite materials.[4] Mg-Ti-H, however, has the great advantage of being switchable. The switching between the two optical states is fast, robust, and reversible. The combination of these properties highlights the applicability of Mg-Ti-H thin films as switchable smart coatings for solar collector applications.[3] Moreover, the fast switching together with the high optical contrast between the reflective and absorbing states makes Mg-Ti-H films also interesting for hydrogen sensor applications.[5] One of the most surprising properties of Mg-Ti-H films is their structural stability. We show here that this is due to the accidental equality of the molar volume of TiH_2 and Mg.

Little is presently known and understood about the structure, stability, bonding, and electronic properties of Mg-Ti alloys or Mg-Ti hydrides. The binary phase diagram of Mg with Ti indicates that no stable bulk compounds are formed. However, based on x-ray diffraction results, it was reported that alloying of Mg and Ti does take place in mechanically alloyed bulk samples[6] and in thin films (physical vapor deposition,[7] e-beam deposition,[1,2] and sputtering[3,8]). On the other hand, the only Mg-Ti-H phase identified so far is Mg_7TiH_x, obtained in bulk alloys by Kyoi *et al.*[9] This phase was synthesized in a high-pressure anvil cell by compressing a mixture of MgH_2 and $TiH_{1.9}$ at 8 GPa and 873 K. However, no Mg_7Ti phase was left after high-temperature dehydrogenation.

In this paper, we investigate the structural, optical, and electrical properties of $Mg_yTi_{1-y}H_x$ thin films obtained by co-sputtering of Mg and Ti at room temperature. Quite remarkably, the crystallinity (as deduced from x-ray diffraction) of the films is preserved during hydrogenation at all intermediate steps. The optical properties vary continuously with metal composition. The structure, on the other hand, is rutile MgH_2 for high Mg content compositions ($y>0.87$) and fluorite otherwise. Combining optical, electrical, and structural data, we find that $Mg_yTi_{1-y}H_x$ is a system made of coherently coupled MgH_2/TiH_2 grains with in addition some x-ray amorphous regions made of insulating MgH_2 and unreacted or partially oxidized Mg and Ti. The structure and the reversibility of Mg-Ti-H make it a unique and interesting material to study the effect of coherence on the reversibility of the hydrogenation process.

II. EXPERIMENT

Mg_yTi_{1-y} thin films are prepared by dc and/or rf magnetron co-sputtering of Mg and Ti on quartz substrates. Various compositions in the $0.55<y<0.95$ range are studied. Typical deposition rates are 2 Å/s for Mg (150 W rf power), 0.1–1 Å/s for Ti (25–160 W dc power), and 1.3 Å/s for Pd (50 W dc power). All the films are covered *in situ* with a Pd layer (5–10 nm) to prevent oxidation of the Mg-Ti film and to promote dissociation of H_2.[10,11] A detailed account of the dissociation mechanism is given by Borgschulte *et al.*[11] Ho-

mogeneous composition and thickness over the entire substrate area are ensured by continuously rotating the substrates during sputtering. In addition, we prepared Mg_yTi_{1-y} ($0.55 < y < 0.95$) gradient thin films to study the concentration dependent properties in a continuous way. The composition of the films is investigated by Rutherford backscattering spectrometry on samples grown in the same deposition run but on carbon substrates. Optical reflection (R) and transmission (T) spectra are measured simultaneously during hydrogenation (pressures up to 1 bar H_2) in a PerkinElmer Lambda 900 diffraction grating spectrometer ($0.495 < \hbar\omega < 6.51$ eV) and a Bruker IFS 66 Fourier transform spectrometer ($0.72 < \hbar\omega < 3.5$ eV). The R-T spectra are measured through the transparent substrate at near normal incidence of the incoming beam. As an indication of hydrogen uptake in the films, the electrical resistivity of the films is measured in a van der Pauw[12] configuration together with the R-T spectra. The structural properties of the films are investigated by means of x-ray diffraction (XRD) in a Bruker D8 Discover x-ray diffractometer equipped with a two-dimensional (2D) detector which can perform real-time diffraction data collection over a large area with high speed, high sensitivity, and low background. A Be dome allows *in situ* x-ray measurements upon hydrogenation. XRD patterns are also measured during dehydrogenation (in air, at room temperature). The dehydrogenation time (few minutes for a 50 nm $Mg_{0.70}Ti_{0.30}$/30 nm Pd film) depends on the thickness of the film and can be improved by decreasing the thickness and/or increasing the temperature.[3,5] All the measurements are done using the Cu $K\alpha$ radiation ($\lambda = 1.5418$ Å). Additionally, transmission electron microscope (TEM) plan-view and cross-sectional images were recorded using a JEOL 2010F working at 200 kV (point resolution of 0.23 nm and information limit of 0.11 nm). This TEM is also equipped with an energy dispersive x-ray spectrometer and a Gatan imaging filter (GIF 2000). The plan-view samples were obtained by directly depositing the films on silicon nitride membranes (30 nm thick). Hydrogenated samples were prepared using a 1 nm Pd cap layer. Cross-section samples were made by cutting, polishing, and ion milling with 4 kV Ar ions with a Gatan precision ion polishing system. To measure the hydrogen content, electrochemical measurements (loading and/or unloading) are done in a standard three electrode setup containing a Hg/HgO reference electrode and a Pt counterelectrode in a 1M KOH electrolyte. The reflection and the transmission at $\lambda = 635$ nm (1.95 eV) can be measured simultaneously in the electrochemical setup.[13,14]

III. RESULTS

A. Optical and electrical properties

Hydrogen uptake in Mg_yTi_{1-y} thin films is fast and induces a gradual change in optical appearance for all alloy compositions. The color of the fully hydrogenated films changes from dark gray to yellowish with increasing Mg fraction. The kinetics of hydrogen uptake improves with increasing Ti content in the alloy[3] and compositions with only a few percents of Ti are already far superior to pure Mg.

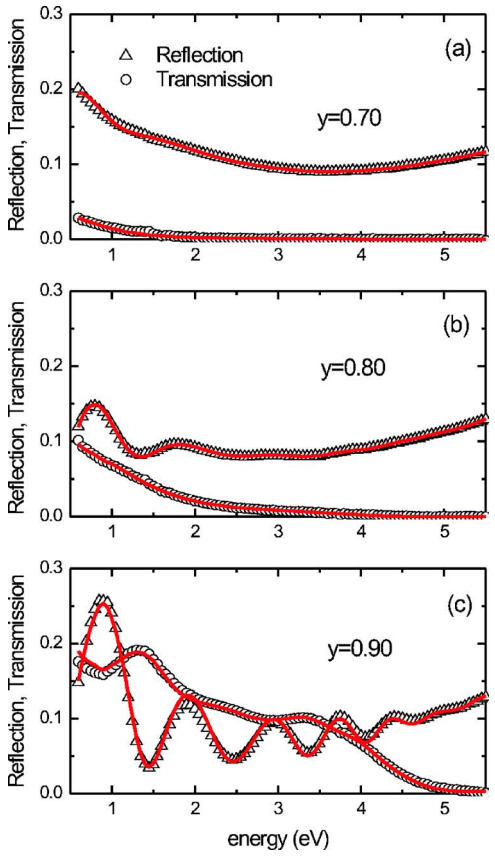

FIG. 1. (Color online) Optical reflection (measured through the substrate) and transmission spectra measured on 200 nm Mg_yTi_{1-y}/10 nm Pd films ($y=0.70$, $y=0.80$, and $y=0.90$) after hydrogenation in 1 bar H_2 at room temperature. The solid lines are calculations using a Drude-Lorentz parametrization scheme.

Reflection and transmission spectra are measured on 200 nm Mg_yTi_{1-y}/10 nm Pd films ($y=0.90$, 0.80, and 0.70) during hydrogenation in 1 bar H_2 at room temperature. In the metallic state (not shown), all the films have zero transmission and a relatively high and featureless reflection that decreases with increasing Ti content. After hydrogen absorption, the reflection is low for all compositions, whereas significant transmission is observed only for the $y=0.90$ sample. The combination of low reflection and low transmission in the hydrogenated state ($y=0.80$ and 0.70 samples) gives rise to a highly absorbing state that extends over the entire visible range. In Fig. 1, the experimental spectra are shown together with calculated spectra using a Drude-Lorentz parametrization scheme. The good agreement shows that the optical properties are consistent with a homogeneous layer. Additional measurements are done on similar compositions but much thinner layers (50 nm) capped with 5 nm Pd. The R-T pectra measured on hydrogenated films are shown in Figs. 2(a) and 2(b). In comparison with the thick films, we measure the same low reflection but much more transmission. These results are similar to those obtained by Farangis *et al.*[15] on amorphous Mg-Ti-H thin films and show that the absorption ($A = 1 - R - T$) of a Mg-Ti-H layer can be tuned just by varying the film thickness. Some insight into the optical transitions can be gained from the energy dependence of the

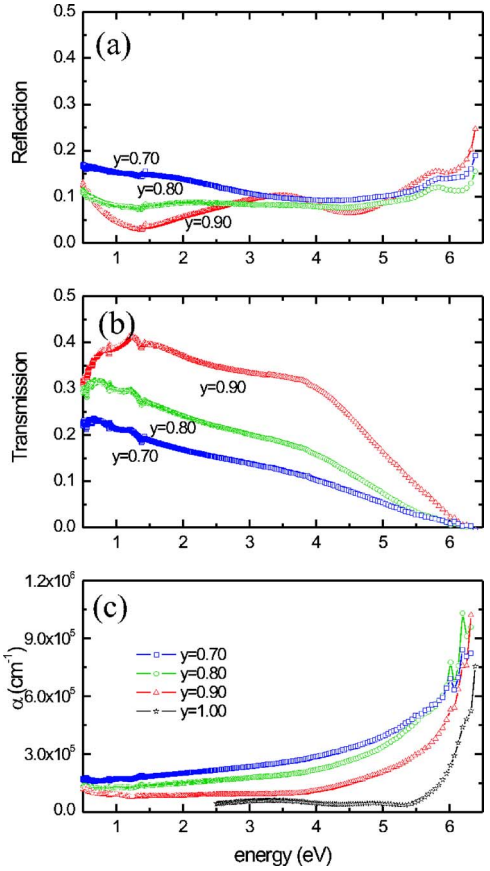

FIG. 2. (Color online) Optical (a) reflection and (b) transmission spectra measured on 50 nm Mg_yTi_{1-y}/5 nm Pd (y=0.70, 0.80, and 0.90) films after hydrogenation in 1 bar H_2 at room temperature. (c) Absorption coefficient α for $Mg_yTi_{1-y}H_x$ (y=0.70, 0.80, 0.90, and 1).

absorption coefficient α. This is calculated from the R-T data measured on thin films and corrected for the Pd cap layer as follows:

$$\alpha = -\frac{1}{d}\left[\ln\left(\frac{T}{1-R}\right) + \alpha_{\mathrm{Pd}} d_{\mathrm{Pd}}\right], \tag{1}$$

with $\alpha_{\mathrm{Pd}}=2k\omega/c$, where k is the extinction coefficient of Pd.[16] The results are shown in Fig. 2(c). For comparison, the absorption coefficient of MgH_2 is also shown. All Mg-Ti-H compositions have a similar dependence: an absorption edge at high energies and significant absorption below this edge. An effective band gap E_g is tentatively estimated by linearly extrapolating the absorption edge to zero. This extrapolation is, however, not unique, making the value of E_g only approximate. The dependence of absorption coefficient on energy is also common to other Mg-based systems such as Mg-Pd-H,[17] Mg-Y-H,[18] or Mg-Ni-H,[19] but the mechanism responsible for this effect is often different. Whereas in Mg-Pd-H it was understood by considering Pd as a deep donor in semiconducting MgH_2, in Mg-Y-H it was attributed to quantum confinement effects. However, such an absorption edge could be seen as the signature of MgH_2 or a phase with a similarly large energy gap.

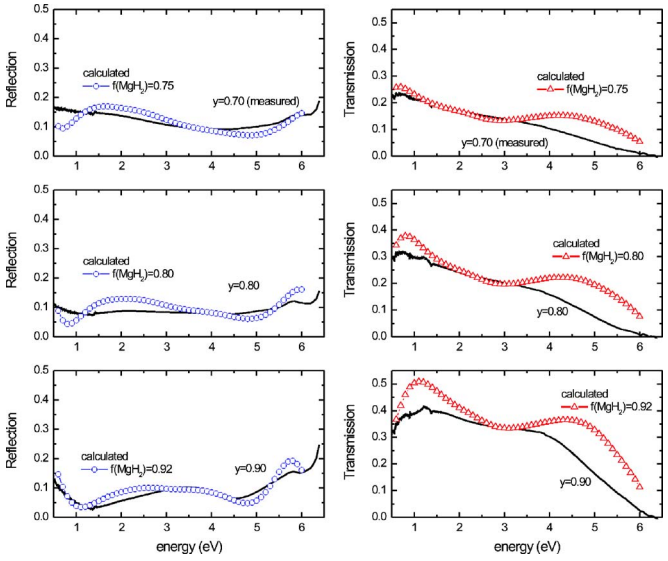

FIG. 3. (Color online) Comparison between reflection and transmission spectra measured on 60 nm $Mg_yTi_{1-y}H_x$/6 nm PdH_x films and spectra calculated assuming a mixture of spherical particles of metallic TiH_2 and semiconducting MgH_2 [volume fraction $f(MgH_2)$].

To get a qualitative understanding of the optical properties, we analyze the optical data within the framework of an effective-medium approximation. We assume a two phase system consisting of a metallic and a dielectric phase. This method was successfully applied previously[20] to the Mg-MgH_2 system to explain that the highly absorbing state found at intermediate hydrogen compositions was due to the coexistence of nanoscale grains of metallic Mg and insulating MgH_2 (with a gap E_g=5.6 eV). The Bruggeman effective-medium approximation[21] can be used if the particle size is smaller than the wavelength of light, a criterion generally valid for metal hydride thin films. As a first approximation of the Mg-Ti-H system, we assume a medium consisting of spherical grains of metallic TiH_2 and insulating MgH_2 [volume fraction $f(MgH_2)$]. The effective dielectric function of such a medium is calculated from the dielectric functions of TiH_2 and MgH_2, determined in separate runs. Subsequently, the transfer-matrix method[22] is used to calculate the reflection and transmission of the total sample also taking into account the quartz substrate and a 6 nm PdH_x cap layer.[16] A comparison with spectra measured on 60 nm $Mg_yTi_{1-y}H_x$/6 nm PdH_x films is shown in Fig. 3. The $f(MgH_2)$ volume fractions used are 0.75, 0.85, and 0.92 for y=0.70, 0.80, and 0.90, respectively. As shown here, the agreement is reasonable below 4 eV, but the calculated data deviate considerably from the measured spectra at high energies. We also considered a nonspherical shape of the grains or even a different effective-medium approximation (e.g., Maxwell-Garnet). In this case, the deviation between the calculated and the measured spectra was even bigger. The failure of an effective-medium approximation to reproduce in detail the measured optical properties indicates a more complex phase composition and/or interaction on an atomic level between the components. However, this analysis indicates unambiguously that the hydrogenated films contain a signifi-

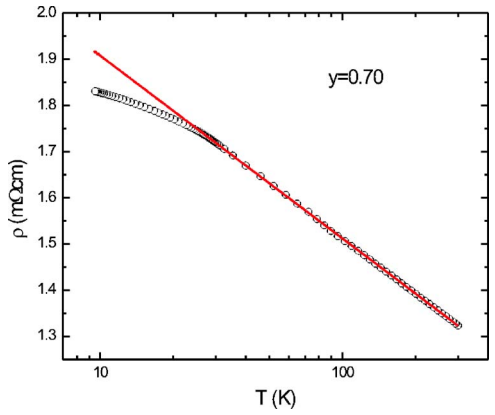

FIG. 4. (Color online) Resistivity versus T (on a logarithmic scale) measured for a 200 nm $Mg_{0.70}Ti_{0.30}$/1 nm Pd film in the fully hydrogenated state (in 1 bar H_2). The solid line is a guide for the eyes.

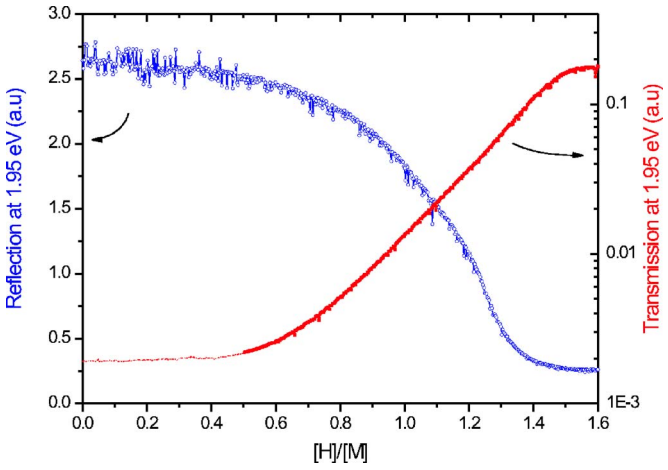

FIG. 5. (Color online) Optical reflection and transmission of a 100 nm $Mg_{0.70}Ti_{0.30}$ film capped with 10 nm Pd measured *in situ* during galvanostatic loading (current $I=-133.3\ \mu A/cm^2$). [H]/[M] corresponds to the number of hydrogen atoms per metal atom. In the region indicated by the dashed line, the measured transmission falls below the sensitivity limit of the instrument.

cant fraction of an insulating material such as MgH_2. This conclusion is further substantiated by electrical resistivity measurements.

As-prepared films have electrical resistivity (ρ) values typical for metals (50–100 $\mu\Omega$ cm). Upon hydrogenation, ρ increases gradually to final values that are more than a factor of 5 higher than in the as-prepared state. Typical values measured on fully hydrogenated films are 1.32 and 1.9 mΩ cm for $y=0.70$ and $y=0.90$ samples, respectively [all the values are corrected for the Pd cap layer by assuming a parallel resistor model and $\rho_{Pd}=0.75\ \mu\Omega$ cm (Ref. 20)]. These values point to a decrease in the number of free carriers in the films. Temperature dependent resistivity measurements done on a 200 nm $Mg_{0.70}Ti_{0.30}$/1 nm Pd sample in the fully hydrogenated state are shown in Fig. 4. Such a thin Pd cap layer is sufficient for hydrogenation of the film but consists of disconnected islands. It is thus possible to measure the intrinsic electrical resistivity of the Mg-Ti layer. Upon cooling, the electrical resistivity increases, pointing to a nonmetallic behavior. The logarithmic temperature dependence of the resistivity in the range of $35\ K<T<298\ K$ is similar to that reported for granular niobium nitride cermet films.[23] A similar dependence was also reported for $YH_{3-\delta}$ (Ref. 24) and discussed in terms of 2D weak electron localization or Kondo scattering. Although the microscopic origin of the $\log T$ dependence in Fig. 4 has not been identified yet, the data imply clearly that $Mg_{0.70}Ti_{0.30}H_{1.55}$ is neither a metal nor a semimetal.

The hydrogen concentration dependence of the optical properties can be obtained from measurements in an optical-electrochemical cell. In this case, reflection and transmission at 1.95 eV are measured simultaneously with the hydrogen content. The results obtained for a 100 nm $Mg_{0.70}Ti_{0.30}$/10 nm Pd film in a constant current mode ($I=-133.3\ \mu A/cm^2$) are shown in Fig. 5. With increasing amount of hydrogen in the sample, the reflection decreases while the transmission increases gradually. Such a behavior is typical for a homogeneous nucleation and growth of a hydride phase within the whole volume of the sample as was observed in Mg-MgH_2 thin films.[20] For $[H]/[M]<0.5$ (dashed line in Fig. 5), the measured transmission falls below the detection limit of the instrument. Above $[H]/[M]>0.5$, the logarithm of the transmission increases linearly as expected from Lambert-Beers's law. The total amount of hydrogen that can be incorporated is $[H]/[M]\sim 1.55$. This value is below the theoretical limit of $[H]/[M]=2$ expected for an alloy of two metals forming the dihydrides TiH_2 and MgH_2. Our results are in agreement with the results of Vermeulen *et al.*[2] measured on e-beam deposited thin films. They moreover showed that the H content in the fully hydrogenated state decreases with increasing the amount of Ti for all alloy compositions measured.

B. Structural properties

Structural data obtained from x-ray diffraction measurements are summarized in Fig. 6. X-ray θ-2θ scans measured on $y=0.70$ and $y=0.90$ samples are shown in Figs. 6(a) and 6(b), respectively. Here, we compare spectra corresponding to the as-prepared (initial), fully hydrogenated (at room temperature in 1 bar H_2), and dehydrogenated (after exposure to air) states.

In the XRD spectra, there are reflections from the Mg-Ti layer and from the Pd cap layer. The peak at $\sim 40.1°$ corresponds to the (111) reflection of Pd. Upon hydrogenation, the peak shifts to lower scattering angles, indicating thus the formation of PdH_x. The reflection of Pd is absent for samples with a composition $y=0.90$, even though the presence of Pd was confirmed by Rutherford backscattering spectroscopy. A similar result was obtained for e-beam deposited Mg-Ti films[1] or pure Mg films.[20] Therefore, on Mg-rich surfaces, the Pd appears not to have a preferential orientation, which is necessary for these thin films to produce an XRD reflection. Very likely, this is related to the morphology of the Mg-Ti and Mg layers.

For as-prepared $y=0.70$ and $y=0.90$ samples [Figs. 6(a) and 6(b)], there is only one reflection peak that is assigned to

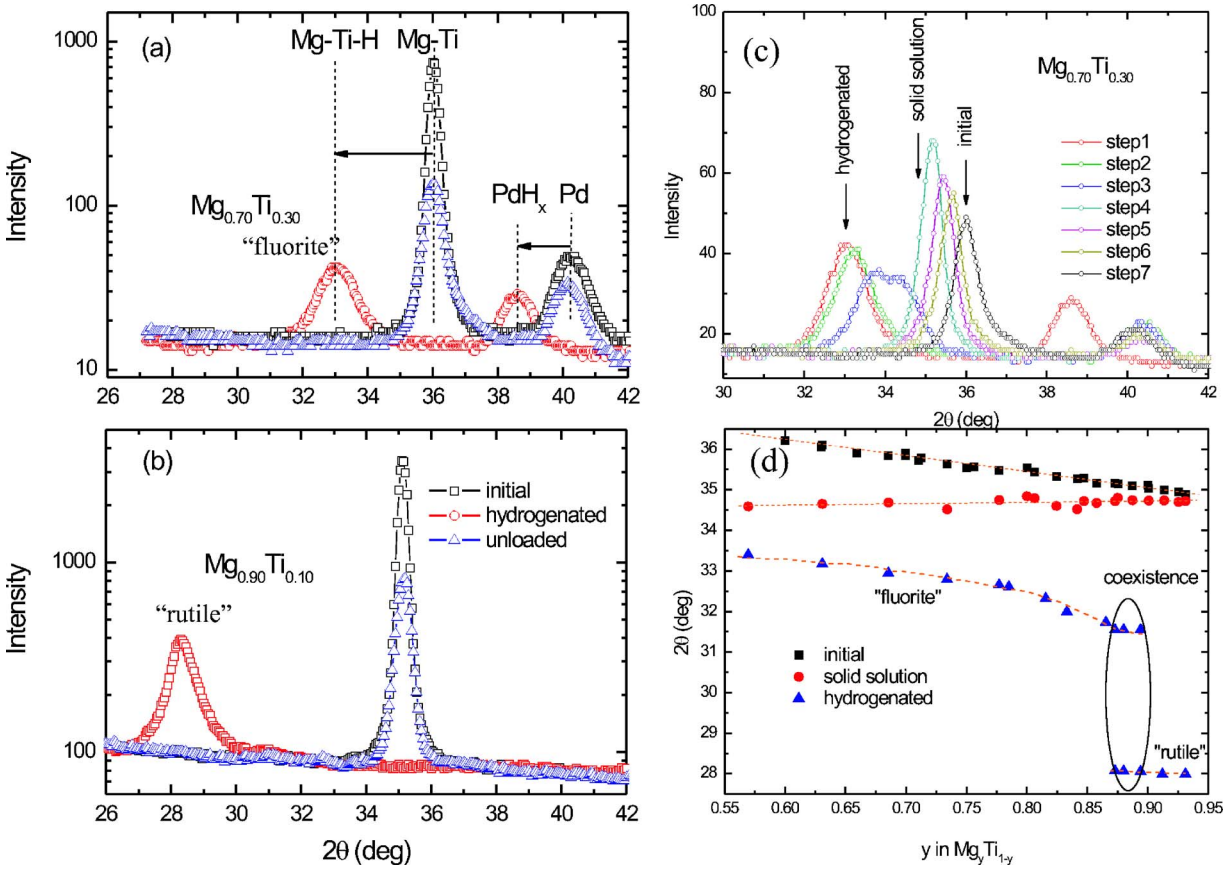

FIG. 6. (Color online) [(a) and (b)] θ-2θ x-ray scans measured on 200 nm Mg_yTi_{1-y}/10 nm Pd films (y=0.70 and y=0.90) in the as-prepared (initial), fully hydrogenated (at room temperature in 1 bar H_2), and fully dehydrogenated states. (c) Intermediate steps during dehydrogenation measured on a y=0.70 sample. (d) Composition dependence of 2θ measured on a Mg_yTi_{1-y} gradient thin film with $0.55 < y < 0.95$. Data corresponding to as-prepared (initial), solid solution (intermediate), and hydrogenated (final) states as defined in (c) are shown.

the Mg-Ti layer. The 2θ position of this peak depends on the Mg/Ti ratio and is between the (002) reflection of Mg (2θ =34.4°; hexagonal structure) and the (002) reflection of Ti (2θ=38.52°; hexagonal structure). This suggests the formation of a Mg-Ti random alloy on deposition with the same hexagonal symmetry as the metal constituents. The formation of a random alloy is, however, highly unlikely given the large positive enthalpy of mixing calculated for such an alloy [>30 kJ/g atom (Ref. 25)]. Instead we argue that, in fact, a coherently coupled mixture of Mg and Ti is formed. The hexagonal symmetry is confirmed by additional TEM plan-view measurements. A typical result measured on a 50 nm $Mg_{0.70}Ti_{0.30}$/5 nm Pd film is shown in Fig. 7(a). The reflections from the Pd cap layer (diffuse rings due to very small crystallites on the order of 5 nm) can easily be distinguished from those of the Mg_yTi_{1-y} film (well defined rings with individual spots due to crystallites on the order of 50 nm). The reflections from the film are consistent with a $P6_3/mmc$ structure (the same as for Mg and Ti) with lattice spacings (a=3.11 Å, c=4.98 Å) in close agreement with the XRD results.

After hydrogenation, we find a reflection at 2θ=28.1° for the y=0.90 sample, whereas for the y=0.70 sample the hydride peak appears at 2θ=32.8°. The difference in peak position suggests a difference in structure of the hydride phase. We can clearly identify the peak at 2θ=28.1° as the (110) reflection of a rutile MgH_2 phase (2θ=27.91° for pure MgH_2). The small shift can be due either to small Ti doping in MgH_2 or to strain in the thin film. On the other hand, the peak at $2\theta \approx 32.8°$ is more difficult to identify. We assume this hydride to have fcc symmetry ("fluorite" phase) as its peak position is close to the (111) reflection of fcc TiH_2 and almost coincides with high-pressure fcc MgH_2.[26] Assuming a fluorite phase, the corresponding lattice spacing is a =4.729 Å. TEM plan-view measurements on hydrogenated $Mg_{0.70}Ti_{0.30}$ films confirm the fcc symmetry [where the (111), (200), (220), (311), and (222) reflections can be identified] and indicate a structural homogeneity at least on a scale above 20 nm [Fig. 7(b)]. The lattice spacing obtained from these measurements is a=4.55 Å. This value is slightly lower than the data obtained from XRD on similar compositions, indicating a partial dehydrogenation due to electron-beam bombardment during the TEM measurements.

The reflection at $2\theta \approx 32.8°$ is also close to the 222 reflection reported for the Mg_7TiH_x phase[9] (Ca_7Ge-type structure; a=9.532 Å) synthesized in a high-pressure anvil cell by mixing MgH_2 and $TiH_{1.9}$ at 8 GPa and 873 K. The structure of this phase was argued to be similar with that of $TiH_{1.9}$ (fcc) but with most of the Ti atoms substituted by Mg in an or-

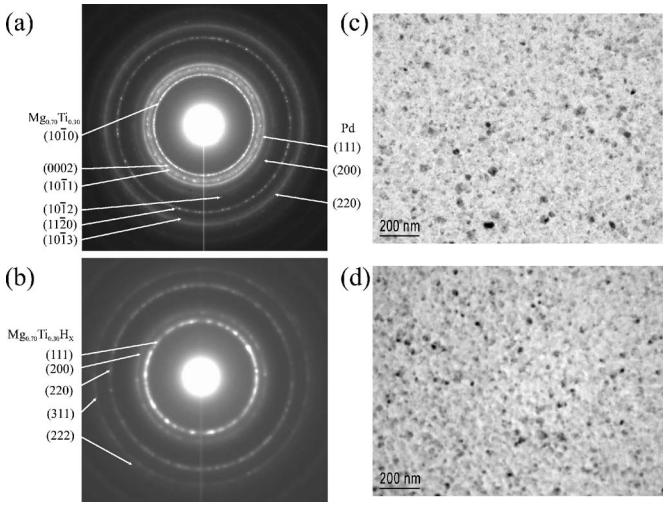

FIG. 7. Selected area electron-diffraction patterns (a) of a $Mg_{0.70}Ti_{0.30}$/5 nm Pd thin film and (b) of a $Mg_{0.70}Ti_{0.30}H_x$/1 nm Pd thin film. Arrows identify reflections from the film (Mg-Ti or Mg-Ti-H) and the Pd cap layer [only visible in (a); in (b) the layer is too thin]. The corresponding TEM plan-view images of the film surface are shown in (c) and (d).

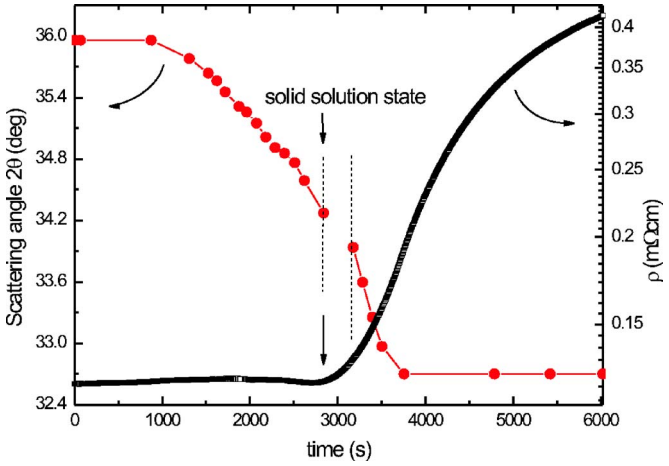

FIG. 8. (Color online) Scattering angle 2θ and electrical resistivity ρ evolution in time during hydrogenation measured simultaneously on a 200 nm $Mg_{0.70}Ti_{0.30}$/10 nm Pd sample. Hydrogenation is done at room temperature in 100 mbar H_2.

dered way, resulting in a superstructure with a doubled unit cell.

As shown in Figs. 6(a) and 6(b), after full dehydrogenation, the peak shifts back to its initial position, which is evidence for the structural reversibility of the system and the absence of phase segregation. This is a surprising result since hydrogen cycling in Mg-based systems is in general accompanied by a large scale phase segregation.[20,27] Also remarkable is the fact that the films remain crystalline during hydrogenation and subsequent dehydrogenation. However, the crystallinity of the films decreases upon hydrogen cycling. This has, however, little effect on the switching time and the optical response[3,5] and therefore we conclude no major structural changes to take place apart from a reduction in grain size.

To understand the structural transformations and its composition dependence, we performed XRD measurements at intermediate stages during hydrogenation (dehydrogenation) on homogeneous samples and also on a Mg_yTi_{1-y} gradient sample with $0.55<y<0.95$. In Fig. 6(d), we have summarized results as measured on the gradient sample. We find that the position of the Mg-Ti peak varies linearly with Mg/Ti ratio [Fig. 6(d)] for the entire composition range. This is in accordance with Vegard's law.[28] A small reflection from Ti is only found for $y<0.65$ compositions but no signs of crystalline Mg are present for all $0.55<y<0.95$ compositions. The XRD data suggest that the alloy has always the hexagonal symmetry, which was confirmed by TEM plan-view measurements on one composition. The results in Fig. 6(d) suggest three distinct structural regimes for the hydrogenated state as a function of composition: (I) single phase fluorite for $y<0.87$, (II) single phase rutile for $y>0.90$, and (III) two phase coexistence for $0.87<y<0.90$. Within the fluorite regime, the structure varies continuously with composition. At intermediate compositions, coexistence of both phases is found. For all compositions, the full width at half maximum indicates very small crystallites on the order of 10–20 nm. As shown in Fig. 6(c), for a $y=0.70$ sample, the transformation between the initial and the hydrogenated state is almost continuous and fully reversible. The intermediate steps shown here are measured during H desorption. Assuming an hcp structure in the as-prepared state and fcc structure in the final state, the intermediate steps should reveal an hcp-fcc phase transformation. Upon H uptake, first the lattice expands continuously (steps 4–7). We define as the solid solution state the whole range of 2θ values which are attained continuously starting from the metallic state. At intermediate hydrogen concentrations (step 3), the double-peak structure of the XRD spectrum points to coexistence of two phases: an fcc phase and an hcp phase. Subsequent H uptake leads to a further expansion of the fcc phase.

Similar intermediate steps can be defined for all compositions in the $0.55<y<0.95$ range. Interestingly, the minimum 2θ angle in the metal solid solution phase is the same for all compositions and corresponds to the scattering angle of both TiH_2 (111 reflection) and Mg (002 reflection). This result strongly suggest a hydrogenation sequence where hydrogen first occupies Ti-related sites in the Mg-Ti lattice. An indication in favor of this scenario is also the increase in peak intensity in the beginning of the hydrogenation process. The lattice expands and becomes more ordered since the molar volume of TiH_2 (13.3 cm^3) equals almost exactly that of pure Mg (13.98 cm^3). The data in Fig. 6(d) also suggest that the amount of hydrogen that can be dissolved as a solid solution in the metal alloy phase increases with increasing Ti concentration.

Additional information on the phase composition of hydrogenated films is obtained from combined structural and electrical resistivity measurements. Results measured on a $y=0.70$ sample are shown in Fig. 8. In the beginning of the hydrogenation process, the electrical resistivity varies only slightly, while 2θ decreases continuously, up to the solid solution state. An increase in electrical resistivity is measured only on further hydrogenation ($t>3000$ s), while 2θ de-

creases further. However, for $t>4000$ s, 2θ remains constant, whereas the electrical resistivity varies almost by a factor of 2. This result suggests the presence of a noncrystalline component that takes up hydrogen. The origin of this phase is not yet clear. It could be related to x-ray amorphous material formed at grain boundaries. A precise estimate of the amount of this phase is rather difficult also because we cannot exclude the formation of crystalline material while the XRD peak remains at a constant position. Hence, the increase in resistivity could also be related to more and more crystalline hydrided material being formed. If we assume only a linear increase of electrical resistivity with hydrogen content and combine the results in Fig. 8 with hydrogen content measurements (see Fig. 5), we can estimate the maximum fraction of amorphous phase to be ~45% of the total for a $y=0.70$ sample. This fraction is quite high and is probably overestimated since TEM plan-view measurements on as-prepared films do not show evidence of an amorphous phase. Very likely, the assumption of a linear increase of electrical resistivity with hydrogen content is too simplistic and possible; crystalline material is still being formed while the XRD peak remains at a constant position. Only on a hydrogen cycled sample, TEM cross-section images and XRD indicate clearly an increase in disorder in comparison to the as-prepared state.

IV. DISCUSSION

As suggested in the previous section, the formation of a Mg-Ti random alloy on deposition is very unlikely given the large positive enthalpy of mixing. The occurrence of a single hcp Bragg pattern is not sufficient to prove the alloy formation on an atomic scale[29,30] but it suggests a certain local order. The reversibility of the hydrogenation process suggests that this ordering remains intact on cycling. The optical and electrical data on fully hydrogenated films suggest the presence of an insulating MgH_2-like phase for all metal alloy compositions. Besides the insulating component, a second phase with a metallic character should be present to account for the highly absorbing state. For example, for a $y=0.70$ sample, the volume fraction of the insulating component is ~75%, corresponding thus to the entire Mg fraction in the metal alloy. In a Mg_yTi_{1-y} homogeneous random alloy, the amount of Mg_4 clusters (equal to y^4 assuming a binomial distribution) is only ~24%, much lower than what is needed to explain the optical and electrical properties. Also on the basis of XRD data, large scale segregation is excluded. Clear structural indications of a rutile MgH_2 phase are found only for Mg-rich compositions ($y>0.87$). For $y<0.87$ compositions, the XRD data point to a structure with cubic symmetry and a lattice parameter that varies continuously with metal composition in the parent alloy.

Recent theoretical calculations on $Mg_{0.75}Ti_{0.25}H_2$ (Ref. 31) structures with a cubic symmetry reveal a metallic character, in disagreement with our temperature dependent resistivity measurements and the optical data. From this and the continuous dependence of structure on metal alloy composition, we conclude that the $Mg_yTi_{1-y}H_x$ films with $y<0.87$ are neither single phase nor phase separated. Instead, the experimental evidence suggests the formation of insulating MgH_2 and metallic TiH_2 regions that form a coherent crystalline structure. This conclusion is consistent with a hydrogenation sequence where hydrogen first occupies Ti-related sites. A schematic representation of a coherent crystalline grain consisting of a Mg and Ti region is shown in Fig. 9(a). The local deformation is only schematic and might deviate from reality. The same crystalline grain after hydrogen uptake in the Ti-related sites and in the fully hydrogenation state is shown in Figs. 9(b) and 9(c), respectively. This peculiar hydrogenation sequence is related to the more negative enthalpy of formation of TiH_2 (−70 kJ/mol H) as compared to MgH_2 (−32 kJ/mol H). Very likely, hydrogenation of Ti-related sites in the beginning of the hydrogenation process reduces the mobility of atoms during further hydrogen uptake and thus prevents the large scale segregation, observed in many other Mg-based systems.

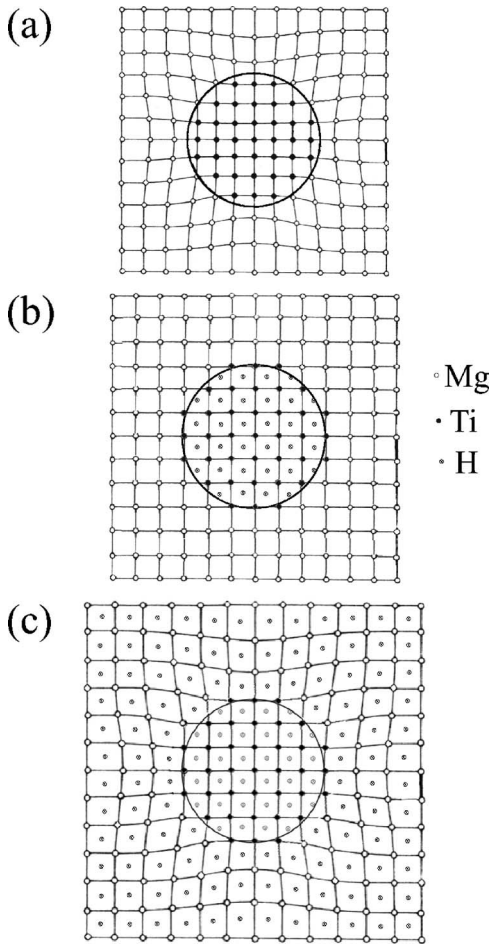

FIG. 9. (a) Schematic representation of a coherent crystalline grain consisting of a Mg and Ti region. (b) The same crystalline grain after hydrogen uptake in the Ti-related sites. (c) Full hydrogenation state. The accidental equality of the molar volumes of TiH_2 and Mg leads to an almost perfect crystal in situation (b).

In a scenario based on a coherent mixture of MgH_2 and TiH_2, the structural data for $y<0.87$ compositions can be understood by assuming that both components have a cubic structure. This is expected for TiH_2. On the other hand, at normal pressures and temperatures, MgH_2 crystallizes in a

rutile structure. A cubic MgH_2 phase was reported to be formed only at high pressures (4 GPa).[26] The theoretical calculations of Vajeeston *et al.*[32] confirm a similar cubic phase as being the most stable structure if the unit-cell volume is reduced to 27.5 Å/f.u. (equivalent to $a=4.79$ Å). The formation of a cubic MgH_2 phase in our thin films, at normal pressures and temperatures, is not entirely clear. Very likely, it is related to the coherent coupling to Ti/TiH_2 and the local stress induced. Using the pressure vs volume dependence calculated by Vajeeston *et al.*[32] the lattice constant of cubic MgH_2 at normal pressures should be $a(MgH_2)=4.839$ Å. With this value, the average lattice spacing of fully hydrogenated Mg_yTi_{1-y} films with $y<0.80$ is well reproduced by the weighted average of the two components as follows

$$a_{Mg_yTi_{1-y}H_x} = ya_{MgH_2} + (1-y)a_{TiH_2}. \quad (2)$$

Then, on average, the hydrogen-to-metal ratio of the crystalline coherent structure is 2. This value corresponds to a higher hydrogen content than what we measured electrochemically ([H]/[M]=1.55), and therefore supports the conclusion that an x-ray amorphous component is present which reacts only partly with hydrogen. Since the optical data suggest a high fraction of insulating material, part of this amorphous component must be insulating with properties similar to those of MgH_2. The rest is likely to remain metallic as unreacted or partially oxidized Mg and Ti. Very likely, this amorphous component does not play an active role in maintaining the coherence of the system.

Structural coherence was reported for several systems with positive energy of mixing, such as Ag-Cu,[33] Cu-Cr,[29] or Cu-Fe,[34] but the mechanism responsible for this effect is still a subject of controversy.[35–38] Experimental results from nanometer-resolution methods such as atom probe field ion microscopy[30] or extended x-ray absorption fine structure could shed more light on the subject. It is though quite remarkable that in Mg-Ti, the coherent structure is preserved at all intermediate states during hydrogenation. This is likely to be related to the similarities in molar volume between Mg and TiH_2.

Recently, the thermodynamic properties of Mg_yTi_{1-y} thin films were studied with hydrogenography.[39] In this method, the equilibrium pressure and the enthalpy of formation of $Mg_yTi_{1-y}H_x$ are determined by following the changes in optical transmission upon hydrogenation. In the $0.65<y<0.90$ range, the enthalpy of formation determined with this method does not depend significantly on composition and is similar to that of thin-film MgH_2. Therefore, these results support our model that considers a coherent structure containing MgH_2.

V. CONCLUSIONS

Hydrogenation of Mg_yTi_{1-y} thin films prepared by cosputtering of Mg and Ti is monitored continuously optically, electrically, and with x-ray diffraction. All the properties are found to depend on the metal ratio in the parent alloy. Structurally, as-prepared films show only one crystalline phase over a wide composition range ($0.55<y<0.95$) that corresponds to a hexagonal Mg-Ti alloy. Hydrogenation induces a reversible phase transformation. The structure of the hydride depends on the metal ratio in the parent alloy. From XRD, the average structure resembles the rutile MgH_2 phase for high Mg content samples ($y>0.90$) and is fluorite otherwise ($y<0.87$). At intermediate composition, coexistence of both phases is found. Highly reflective in the metallic state, the films are highly absorbing in the fully hydrogenated state (87% of the solar spectrum for $Mg_{0.80}Ti_{0.20}H_x$). Such a highly absorbing state hints at the coexistence of a metallic and a semiconducting phase. It is, however, not simply a composite material consisting of independent MgH_2 and TiH_2 grains. By continuously monitoring the structure during H uptake, we obtain data that are compatible with a coherent structure. The complete reversibility of the system and the structural coherence are probably related to the equality of the molar volumes of TiH_2 and Mg. The present results point toward a rich and unexpected chemistry of Mg-Ti-H compounds.

ACKNOWLEDGMENTS

This work is part of the research program of the Stichting voor Fundamenteel Onderzoek der Materie (FOM) and the Technologiestichting STW. Both are financially supported by the Nederlandse Organisatie voor Wetenschappelijk Onderzoek (NWO). Partial funding by the European Commission DG Research (Contract No. SES6-2006-518271, NESSHY) is gratefully acknowledged by the authors.

*Corresponding author. Email address: dborsa@nat.vu.nl

[1] R. A. H. Niessen and P. H. L. Notten, Electrochem. Solid-State Lett. **8**, A534 (2005).
[2] P. Vermeulen, R. A. H. Niessen, and P. H. L. Notten, Electrochem. Commun. **8**, 27 (2006).
[3] D. M. Borsa, A. Baldi, M. Pasturel, H. Schreuders, P. Vermeulen, P. H. L. Notten, B. Dam, and R. Griessen, Appl. Phys. Lett. **88**, 241910 (2006).
[4] S. Shuxi and E. Wäckelgård, Sol. Energy Mater. Sol. Cells **90**, 243 (2006).
[5] M. Slaman, B. Dam, M. Pasturel, D. M. Borsa, H. Schreuders, J. H. Rector, and R. Griessen, Sens. Actuators B **123**, 538 (2007).
[6] G. Liang and R. Schulz, J. Mater. Sci. **38**, 1179 (2003).
[7] T. Mitchell, S. Diplas, P. Tsakiropoulos, J. F. Watts, and J. A. D. Matthew, Philos. Mag. A **82**, 841 (2002).
[8] P. Vermeulen, R. A. H. Niessen, D. M. Borsa, B. Dam, R. Griessen, and P. H. L. Notten, Electrochem. Solid-State Lett. **9**, A520 (2006).
[9] D. Kyoi, T. Sato, E. Rönnebro, N. Kitamura, A. Ueda, M. Ito, S. Katsuyama, S. Hara, D. Noréus, and T. Sakai, J. Alloys Compd. **372**, 213 (2004).
[10] J. N. Huiberts, R. Griessen, J. H. Rector, R. J. Wijngaarden, J. P.

Decker, D. G. de Groot, and N. J. Koeman, Nature (London) **380**, 231 (1996).
[11] A. Borgschulte, R. J. Westerwaal, J. H. Rector, H. Schreuders, B. Dam, and R. Griessen, J. Catal. **239**, 263 (2006).
[12] L. J. van der Pauw, Philips Res. Rep. **13**, 1 (1958).
[13] P. H. L. Notten, M. Kremers, and R. Griessen, J. Electrochem. Soc. **143**, 3348 (1996).
[14] E. S. Kooij, A. T. M. van Gogh, and R. Griessen, J. Electrochem. Soc. **146**, 2990 (1999).
[15] B. Farangis, P. Nachimuthu, T. J. Richardson, J. L. Slack, B. K. Meyer, R. C. C. Perera, and M. D. Rubin, Solid State Ionics **165**, 309 (2003).
[16] *Handbook of Optical Constants of Solids*, edited by E. D. Palik (Academic, San Diego, 1998), Vols. I-III.
[17] M. Pasturel, M. Slaman, H. Schreuders, J. H. Rector, D. M. Borsa, B. Dam, and R. Griessen, J. Appl. Phys. **100**, 023515 (2006).
[18] S. J. van der Molen, D. G. Nagengast, A. T. M. van Gogh, J. Kalkman, E. S. Kooij, J. H. Rector, and R. Griessen, Phys. Rev. B **63**, 235116 (2001).
[19] W. Lohstroh, R. J. Westerwaal, J. L. M. van Mechelen, H. Schreuders, B. Dam, and R. Griessen, J. Alloys Compd. **430**, 13 (2007).
[20] I. A. M. E. Giebels, J. Isidorsson, and R. Griessen, Phys. Rev. B **69**, 205111 (2004).
[21] D. A. G. Bruggeman, Ann. Phys. **24**, 636 (1935).
[22] M. Born and E. Wolf, *Principles of Optics* (Cambridge University Press, Cambridge, 1980).
[23] R. W. Simon, B. J. Dalrymple, D. Van Vechten, W. W. Fuller, and S. A. Wolf, Phys. Rev. B **36**, 1962 (1987).
[24] J. N. Huiberts, R. Griessen, R. J. Wijngaarden, M. Kremers, and C. Van Haesendonck, Phys. Rev. Lett. **79**, 3724 (1997).
[25] F. R. de Boer, R. Boom, W. C. M. Mattens, A. R. Miedema, and A. K. Niessen, *Cohesion in Metals: Transition Metal Alloys* (North-Holland Physics, Amsterdam, 1988).
[26] J. P. Bastide, B. Bonnetot, J. M. Letoffe, and P. Claudy, Mater. Res. Bull. **15**, 1779 (1980).
[27] P. van der Sluis, M. Ouwerkerk, and P. A. Duine, Appl. Phys. Lett. **70**, 3356 (1997).
[28] L. Vegard, Z. Phys. **5**, 17 (1921).
[29] C. Michaelsen, Philos. Mag. A **72**, 813 (1995).
[30] A. Pundt and C. Michaelsen, Appl. Surf. Sci. **87**, 264 (1995).
[31] S. Er (private communication).
[32] P. Vajeeston, P. Ravindran, A. Kjekshus, and H. Fjellvag, Phys. Rev. Lett. **89**, 175506 (2002).
[33] T. Klassen, U. Herr, and R. S. Averback, Acta Mater. **45**, 2921 (1997).
[34] A. R. Yavari, P. J. Desre, and T. Benameur, Phys. Rev. Lett. **68**, 2235 (1992).
[35] G. Veltl, B. Scholz, and H.-D. Kunze, Mater. Sci. Eng., A **134**, 1380 (1991).
[36] A. R. Yavari and P. J. Desre, Mater. Sci. Forum **88-90**, 43 (1992).
[37] H. J. Fecht, E. Hellstern, Z. Fu, and W. L. Johnson, Metall. Trans. A **21A**, 2333 (1990).
[38] C. Gente, M. Oehring, and R. Bormann, Phys. Rev. B **48**, 13244 (1993).
[39] R. Gremaud, C. Broeders, D. M. Borsa, A. Borgschulte, H. Schreuders, J. H. Rector, B. Dam, and R. Griessen (unpublished).